

A Decoupled and Linear Framework for Global Outlier Rejection over Planar Pose Graph

Tianyue Wu and Fei Gao

Abstract—We propose a robust framework for the planar pose graph optimization contaminated by loop closure outliers. Our framework rejects outliers by first decoupling the robust PGO problem wrapped by a *Truncated Least Squares* kernel into two subproblems. Then, the framework introduces a linear angle representation to rewrite the first subproblem that is originally formulated with rotation matrices. The framework is configured with the *Graduated Non-Convexity* (GNC) algorithm to solve the two non-convex subproblems in succession without initial guesses. Thanks to the linearity properties of both the subproblems, our framework requires only linear solvers to optimally solve the optimization problems encountered in GNC. We extensively validate the proposed framework, named *DEGNC-LAF* (*DEcoupled Graduated Non-Convexity with Linear Angle Formulation*) in planar PGO benchmarks. It turns out that it runs significantly (sometimes up to over 30 times) faster than the standard and general-purpose GNC while resulting in high-quality estimates.

I. INTRODUCTION

Pose Graph Optimization (PGO) is a fundamental estimation engine for Simultaneous Localization and Mapping (SLAM) in many robotics actions. The PGO problem finds poses of the robot that best explain the obtained measurements. Typically, the measurements are contaminated by noise and the solution space of the poses to be estimated lies in the special Euclidean group, which makes the PGO problem untrivial.

Despite the challenges of PGO, recently proposed techniques (e.g., SE-Sync [1]) can solve PGO optimally under mild preconditions. However, a portion of loop closure measurements are outliers in practice due to the inevitable perceptual aliasing. In the presence of outliers, even the optimal solution of PGO can still significantly deviate from the ground-truth. Therefore, it is common to use robust PGO techniques [2]–[6] to gain resilience against outliers.

However, the state-of-the-art methods for robust PGO are either *local* [4], implying an over-dependence on a reliable initial guess, or consume heavy computational resources [7], [8] and thus are far from being able to take on a broader range of tasks flexibly. Therefore, it is desirable to develop *global*¹ outlier rejection techniques that often succeed in eliminating the misinformation of outliers while performing considerable efficiency.

In this paper, we show that we can fill the abovementioned gaps in the *planar* PGO setup. Specifically, by decoupling

rotation and translation estimates in planar PGO and adopting an angle setting which uses the orientation angle to represent the rotational component of the robot’s pose, we construct two internally linear subproblems wrapped by the *Truncated Least Squares* (TLS) kernel. We adopt the standard *Graduated Non-Convexity* (GNC) [8], [9] algorithm to solve these two non-convex subproblems. Thanks to the linearity properties of the two subproblems, our proposed framework requires only linear solvers that are lightweight and extremely efficient.

Contribution. Our main contribution is to propose a novel framework to globally reject outliers over planar pose graph with considerable efficiency. The corresponding algorithm, named *DEcoupled Graduated Non-Convexity with Linear Angle Formulation* (DEGNC-LAF), can (i) perform global outlier rejection while exhibiting superior efficiency to general-purpose global methods (e.g., [7], [8]) and (ii) withstand outlier rates that may occur in real-world tasks, thus resulting in high-quality estimates.

Moreover, we propose and validate that the first subproblem in an angle-based setting converges GNC with better accuracy and robustness (and much faster) than the one based on rotation matrix, which results in a significant performance enhancement of the decoupled framework (see *Remark 1* and Section VII).

We extensively validate the proposed approach in standard PGO benchmarks. The results illustrate that DEGNC-LAF is significantly faster than the standard and general-purpose GNC algorithm [8] while usually outperforming or matching GNC and local robust PGO techniques [4], [5] in terms of accuracy and robustness.

II. RELATED WORK

Ideas for designing robust PGO algorithms can be divided into two main categories: (i) mining empirical or statistical evidence of outliers and filtering them out accordingly, and (ii) reformulating to robustify the original PGO problem and solving the reformulated problem.

A. Mining Evidence of Outliers

Latif *et al.* [5] proposed the *Realizing, Reversing, and Recovering* (RRR) algorithm to reject outliers based on the residuals of local PGO. Mangelson *et al.* [6] proposed *Pairwise Consistency Maximization* (PCM) to select the set of inliers, which checks pairwise consistency for each two loop closures and infers the set of inliers from a graphical representation of pairwise consistency. Indelman *et al.* [10] modeled the problem of whether a loop closure is an outlier

All authors are with the State Key Laboratory of Industrial Control Technology, Institute of Cyber-Systems and Control, Zhejiang University, Hangzhou, 310027, China. {modern-gangster, fgaoaa}@zju.edu.cn

¹We identify a method as global if it requires no initial guess or its result is independent of the initial guess.

as a *maximum a posteriori estimation* problem. The authors inferred the formulated problem via *Expectation Maximization* with a good initial guess. A similar idea of using a probabilistic framework to infer outliers can be found in [11].

B. Reformulating to Gain Robustness against Outliers

The existing robust PGO algorithms reformulating to robustify the original problem mainly follow three ways: (i) introducing *switchable variables*, (ii) adopting the *Consensus Maximization* [12], [13] paradigm and (iii) adopting the *M-estimation* [14], [15] paradigm.

1) *Switchable variable*: The formulations proposed in [2]–[4], [16] introduce switchable variables for untrusted edges in the pose graph. For continuous optimization problems with switchable variables (e.g., [2]–[4]), standard nonlinear optimization techniques can be used to solve them. Some off-the-shelf libraries, such as ceres-solver [17] and g2o [18], provide implementations of these techniques. By contrast, the switchable variables in [16] are binary (i.e., discrete), so the alternating minimization framework proposed by the authors was used to solve the problem. Unfortunately, the solving techniques mentioned above are all local, requiring reliable initial guesses.

2) *Consensus Maximization*: Consensus Maximization (CM) looks for an estimate that maximizes the number of measurements with errors under a prescribed threshold. RANSAC [19] is a popular heuristic for CM and requires no initial guess, but the performance of RANSAC is indeterministic and its runtime grows exponentially with increasing outlier rates. Tzoumas et al. [7] proposed ADAPT, a general-purpose heuristic algorithm to solve *Minimally Trimmed Squares* (MTS) estimation which shares commonalities with the CM paradigm [20].

3) *M-estimation*: M-estimation robustifies the original cost function of a problem via wrapping it in a robust kernel. Local nonlinear optimization is an efficient way to solve robust structure from motion (SFM) [21], [22] and robust PGO [23] formulated as M-estimation problems. To get rid of the dependence of robust kernel-wrapped PGO problems on reliable initial guesses, Carlone and Calafiore [24] proposed convex relaxations for the l_1 -norm and Huber kernels. *Graduated Non-Convexity* (GNC) has been used in robust estimation problems [9], [25] as a heuristic to globally solve M-estimation problems. More recently, Yang et al. [8] combined modern global non-minimal solvers (e.g., SE-Sync) with Black-Rangarajan duality [9] and GNC for M-estimation, which benefits our work (see Section V).

III. DECOUPLED ROBUST PLANAR PGO

A. Coupled and Rotation Matrix-based Planar PGO

Planar PGO solves 2D poses (R_i, t_i) sampled along the robot trajectory, where $R_i \in \text{SO}(2)$ and $t_i \in \mathbb{R}^2$. Typically, we anchor the first pose and assume that the noisy measurements $(\tilde{R}_{ij}, \tilde{t}_{ij})$ obtained by the robot are sampled from the following probabilistic generative model [1]:

$$\tilde{R}_{ij} = R_{ij} R_{ij}^\epsilon, \quad R_{ij}^\epsilon \sim \text{Langevin}(I_2, \kappa_{ij}), \quad (1a)$$

$$\tilde{t}_{ij} = t_{ij} + t_{ij}^\epsilon, \quad t_{ij}^\epsilon \sim \mathcal{N}(0, \tau_{ij}^{-1} I_2), \quad (1b)$$

where for all pairwise poses (i, j) , (R_{ij}, t_{ij}) is the true but latent value of relative poses.

Given the noisy measurements and substituted into the probability model of Langevin [26] and Gaussian distribution appearing in (1a) and (1b), the (coupled and rotation matrix-based) PGO is modeled as a *maximum likelihood estimation* problem [1]:

$$(\hat{R}, \hat{t}) = \arg \min_{\substack{R_i \in \text{SO}(2) \\ t_i \in \mathbb{R}^2}} \sum_{(i,j)} \left\{ \begin{aligned} &\kappa_{ij} \| R_j - R_i \tilde{R}_{ij} \|_F^2 \\ &+ \tau_{ij} \| t_j - t_i - R_i \tilde{t}_{ij} \|_2^2 \end{aligned} \right\}, \quad (2)$$

where (\hat{R}, \hat{t}) is a compact representation of the solution to problem (2).

Problem (2) is recently proposed to be tightly relaxed as a (convex) *semidefinite programming* under mild preconditions [1], and thus can be solved optimally. However, in real-world tasks, a fraction of the loop closure measurements are outliers. The original formulation (2) is sensitive to these outliers, so it is common to apply robust kernels to wrap the original problem, which will be introduced in the following subsection.

B. Robust Planar PGO with Truncated Least Squares Kernel

To limit as much as possible the sensitivity of planar PGO to outliers, we adopt the *Truncated Least Squares* (TLS) kernel to reformulate the planar PGO problem (2), which leads to the *Truncated Least Squares Coupled and Rotation Matrix-Based Planar PGO* (TLS-PGO) problem:

$$\min_{\substack{t_i \in \mathbb{R}^2 \\ R_i \in \text{SO}(2)}} \sum_{(i,j) \in \mathcal{E}_{od}} (r_{ij}^{pgo})^2 + \sum_{(i,j) \in \mathcal{E}_{lc}} \rho_c(r_{ij}^{pgo}), \quad (3)$$

where

$$\rho_c(r) = \min(r^2, c^2) \quad (4)$$

is the TLS kernel, \mathcal{E}_{od} and \mathcal{E}_{lc} are the sets consisting of odometry and loop closure respectively, and

$$r_{ij}^{pgo} = \sqrt{\kappa_{ij} \| R_j - R_i \tilde{R}_{ij} \|_F^2 + \tau_{ij} \| t_j - t_i - R_i \tilde{t}_{ij} \|_2^2}. \quad (5)$$

In problem (3) we only apply the TLS kernel to loop closure measurements, while we can typically trust odometry measurements as inliers.

C. Decoupled Robust Planar PGO

In this subsection, we propose a decoupled framework for robust planar PGO. We decouple problem (3) into two subproblems that are solved successively. The subproblem to be solved first is the *Truncated Least Squares Rotation Matrix-Based Planar Rotation Averaging* (TLS-RA) problem:

$$\min_{R_i \in \text{SO}(2)} \sum_{(i,j) \in \mathcal{E}_{od}} (r_{ij}^{ra})^2 + \sum_{(i,j) \in \mathcal{E}_{lc}} \rho_{c_1}(r_{ij}^{ra}), \quad (6)$$

where

$$r_{ij}^{ra} = \sqrt{\kappa_{ij} \| R_j - R_i \tilde{R}_{ij} \|_F^2}. \quad (7)$$

Once problem (5) is solved, the rotation R_i will be fixed in the second subproblem. Thereby, we have the second subproblem, the *Truncated Least Squares Rotation Matrix-Based Planar Translation Averaging (TLS-TA)* problem:

$$\min_{t_i \in \mathbb{R}^2} \sum_{(i,j) \in \mathcal{E}_{od}} (r_{ij}^{ta})^2 + \sum_{(i,j) \in \mathcal{E}_{lc}} \rho_{c2} (r_{ij}^{ta}), \quad (8)$$

where

$$r_{ij}^{ta} = \sqrt{\tau_{ij} \|t_j - t_i - \hat{R}_i \tilde{t}_{ij}\|_2^2}, \quad (9)$$

where \hat{R}_i is the rotation estimate determined by solving problem (6) and remains constant in problem (8).

We note that the estimate obtained by successively optimally solving subproblem (6) and subproblem (8) is not equivalent to the one obtained by optimally solving problem (3). But an important fact is that empirically, the optimal rotation estimate from solving problem (6) is close to the one from solving problem (3). This can be explained by the fact that (i) in the absence of outliers, these two estimates are usually close to each other, as shown in Table 1, and (ii) if problems (3) and (6) are solved optimally in the presence of outliers, the rotation estimates will be more or less close to those in the absence of outliers due to the robustness of the TLS kernel, and thus are close to each other. Therefore, robust rotation estimation does not undergo significant distortion due to decoupling, which leads the translation estimate from optimally solving problem (8) to be consistent with the one obtained from optimally solving problem (3).

IV. ROBUST PLANAR ROTATION ESTIMATION WITH ANGLE-BASED LINEAR FORMULATION

Although rotation matrices can extensively represent planar and spatial rotations without singularity, the planar rotation has another *angle* setting that is less mentioned today but enables the decoupled framework to work better. In this section we show how to use this angle setting to construct a problem to replace the problem (6) in the decoupled framework.

A. Angle Setting of Planar Rotation in Linear Formulation

We use the robot's orientation angle θ_i instead of the rotation matrix to represent the rotational component of the robot's pose, so that the probabilistic generative model of the rotation measurements (i.e., eq. (1a)) is replaced with the following model:

$$\begin{aligned} \tilde{\theta}_{ij} &= \langle \theta_j - \theta_i + \theta_{ij}^\epsilon \rangle = \theta_j - \theta_i + k_{ij} 2\pi + \theta_{ij}^\epsilon, \\ \theta_{ij}^\epsilon &\sim \mathcal{N}(0, \kappa_{ij}^{-1} I_2), \end{aligned} \quad (10)$$

where $\langle \cdot \rangle : \mathbb{R} \rightarrow (-\pi, +\pi]$ is the 2D *geodesic distance* and $k_{ij} \in \mathbb{Z}$ is called a *regularization variable* [27] that regularizes the angle measurements in the interval $(-\pi, +\pi]$.

We now consider the rotation averaging problem in this orientation angle setting when no robust kernel is applied:

$$\min_{\substack{\theta_i \in \mathbb{R} \\ k_{ij} \in \mathbb{Z}}} \sum_{(i,j)} \kappa_{ij} \|\theta_j - \theta_i + k_{ij} 2\pi - \tilde{\theta}_{ij}\|_2^2. \quad (11)$$

TABLE I
AVERAGE ROTATION ERROR (ARE) BETWEEN OPTIMAL SOLUTIONS TO PGO AND ROTATION AVERAGING ON STANDARD DATASETS

| Dataset (no outliers) | ARE (deg) |
|-----------------------|-----------|
| city10000 | 0.6971 |
| intel | 0.9215 |
| kitti_00 | 0.6453 |
| kitti_02 | 0.3268 |
| kitti_05 | 0.1494 |
| manhattan | 0.5306 |
| csail | 0.0631 |

We can clearly see that if the regularization variable k_{ij} can be determined a priori and fixed, we will obtain a *linear estimation* problem from (11), which makes its robust version much less difficult to solve (see *Remark 1*).

We adopt the approximate method proposed in [27] to estimate the regularization variable k_{ij} without solving the integer-mixed problem (11). k_{ij} can be determined based on the fact that in the absence of noise, the measurements $\tilde{\theta}_{ij}$ along each *cycle* in the pose graph have to sum-up to zero, of which a sufficient and necessary condition is that the measurements along each cycle in the *cycle basis* [28] of the pose graph sum-up to zero. According to this fact, the integer k_{ij} can be closed-form solved from a linear system. In the presence of noise, k_{ij} solved from the linear system will no longer be an integer, but the corresponding regularization variable can be rounded to the integer closest to it. This rounding scheme is perfectly accurate in the majority of real-world scenarios [27], so we can convincingly adopt it to determine k_{ij} a priori, thus converting problem (11) into a linear estimation.

B. Robust Rotation Averaging in Angle-Based Setting

By adopting the linear angle setting shown in (11), we can replace problem (6) with the *Truncated Least Squares Angle-Based Planar Rotation Averaging (TLS-ARA)* problem:

$$\min_{\theta_i \in \mathbb{R}} \sum_{(i,j) \in \mathcal{E}_{od}} (r_{ij}^{ara})^2 + \sum_{(i,j) \in \mathcal{E}_{lc}} \rho_{c1} (r_{ij}^{ara}), \quad (12)$$

where

$$r_{ij}^{ara} = \sqrt{\kappa_{ij} \|\theta_j - \theta_i + k_{ij} 2\pi - \tilde{\theta}_{ij}\|_2^2}. \quad (13)$$

Although both problem (12) and problem (6) are non-convex and difficult to solve directly, intuitively, problem (12) will be easier to solve because it is a robust linear estimation problem with *scalar* solution, whereas the solution space of (6) is situated on a matrix manifold [29].

The following section demonstrates how to solve problems (3), (6), (8), (12) using a general GNC framework.

V. SOLVING ROBUST PGO VIA GRADUATED NON-CONVEXITY

Firstly, we note that problems (3), (6), (8), (12) share the uniform form:

$$\min \sum_{(i,j) \in \mathcal{E}_{od}} (r_{ij})^2 + \sum_{(i,j) \in \mathcal{E}_{lc}} \rho_c (r_{ij}), \quad (14)$$

which can be equivalently rewritten as follows:

$$\min \left\{ \sum_{(i,j) \in \mathcal{E}_{od}} (r_{ij})^2 + \sum_{(i,j) \in \mathcal{E}_{lc}} \min_{w_{ij} \in \{0,1\}} [w_{ij} r_{ij}^2 + (1 - w_{ij}) c^2] \right\}. \quad (15)$$

Problem (15) allows the use of (i) *Alternating Optimization* (AM), (ii) *Semidefinite Programming* (SDP) [30] and (iii) *Graduated Non-Convexity* (GNC) [8] to solve it. However, while AM is efficient, it requires an initial guess and can easily fall into local minima. By contrast, SDP can provide optimality certificates, but is very slow to solve at this stage. Therefore, we adopt GNC, which requires no initial guesses and can effectively avoid local minima while performing good efficiency, to solve the problem.

Applying a *GNC function* [9] controlled by a parameter μ to approximate the TLS kernel, GNC uses a *continuation algorithm* [31] to optimize the following problem instead of problem (15):

$$\min \left\{ \sum_{(i,j) \in \mathcal{E}_{od}} (r_{ij})^2 + \sum_{(i,j) \in \mathcal{E}_{lc}} \min_{w_{ij} \in [0,1]} \left[w_{ij} r_{ij}^2 + \frac{\mu(1 - w_{ij})}{\mu + w_{ij}} c^2 \right] \right\}, \quad (16)$$

for which the parameter μ is gradually updated by multiplying a continuation factor f at a time. Intuitively, updating μ implies adjusting the convexity of the kernel that will gradually revert to TLS as μ increases.

GNC is initialized by solving a globally solvable problem, i.e., the optimization problem in the form of (16) with μ tending to zero and all w_{ij} being 1, shown as follows:

$$\min \sum_{(i,j)} (r_{ij})^2, \quad (17)$$

which can be solved optimally with global PGO techniques [1] with r_{ij} specified as r_{ij}^{pgo} (5), global rotation averaging techniques [1], [32] with r_{ij} specified as r_{ij}^{ra} (7) and linear solver with r_{ij} specified as r_{ij}^{la} (9) or r_{ij}^{ara} (13).

The solution to problem (17) is used as the initial guess for the subsequent optimizations in GNC. For each update of μ (called one iteration), GNC alternately optimizes two subproblems of problem (16): the first subproblem optimizes w_{ij} , where r_{ij} is determined by the solution of the second subproblem in the previous iteration, for which a closed-form solution exists (cf. [8]); the second subproblem optimizes r_{ij} , where w_{ij} is determined by the first subproblem in the current iteration. The second subproblem can be considered a weighted version of problem (17) and thus can be solved globally with the same tools. GNC will keep iterating until all w_{ij} become binaries. We can identify a measurement as an outlier if its corresponding w_{ij} converges to 0.

VI. DECOUPLED GRADUATED NON-CONVEXITY WITH LINEAR ANGLE FORMULATION

By introducing the angle setting and GNC algorithm, we proposed a decoupled and linear framework, named *DEcoupled Graduated Non-Convexity with Linear Angle Formulation* (DEGNC-LAF), to globally reject outliers over planar pose graph, the pipeline of which is shown as follows:

- 1) Computing regularization variables k_{ij} in eq. (13)
- 2) Using GNC with k_{ij} to solve TLS-ARA (problem (12)) to obtain the rotation estimate \hat{R}_i
- 3) Using GNC with \hat{R}_i to solve TLS-TA (problem (8)) and rejecting outliers according to the resulting w_{ij} (w_{ij} corresponding to outliers will converge to 0)
- 4) Using SE-Sync with inliers to finally estimate rotations and translations (\hat{R}, \hat{t})

The pseudocode is summarized in Algorithm 1.

We note that instead of taking the solutions to TLS-ARA and TLS-TA as the output estimates, we use the rotation estimates of TLS-ARA to serve for solving TLS-TA and reject outliers based on the resulting w_{ij} of TLS-TA. We end up optimizing poses in coupled PGO using SE-Sync. Such an approach will result in more accurate estimates.

Remark 1 (Benefits of Decoupling and Linear Formulation): Linear formulation (9) and (13) enables the initialization problem (17) and the second subproblem of (16) in the GNC algorithm linearly solvable, thus ensuring that optimal solutions can be obtained. In contrast, in the iterations of solving problem (3) and problem (6), GNC needs to repeatedly call nonlinear global solvers which require preconditions to get the global optimal solution. As a result, the solvers may fail to get the optimal solution in the first few iterations, which increases the risk of GNC falling into local minima. In addition, linear systems can be solved exceptionally efficiently and do not require the computation of optimality certificates which is rather time-consuming.

Algorithm 1: DEcoupled Graduated Non-Convexity with Linear Angle Formulation (DEGNC-LAF)

Input: reduced incidence matrix \mathbf{A} (topology of the pose graph), measurements set $\{(\tilde{R}_{ij}, \tilde{t}_{ij})\}$, noise level sets $\{\kappa_{ij}\}$ and $\{\tau_{ij}\}$, odometry set \mathcal{E}_{od} , loop closure set \mathcal{E}_{lc} , threshold c_1 (default: `chi2inv(0.99, 1)`), threshold c_2 (default: `chi2inv(0.99, 2)`), and GNC continuation factor f (default: 1.4);

Output: inlier indicator \mathcal{I} , poses estimate (\hat{R}, \hat{t})

begin

```

    // Compute regularization variables
     $\{k_{ij}\} \leftarrow \text{Regularize}((\tilde{R}_{ij}, \tilde{t}_{ij}), \mathbf{A});$ 
    // Solve TLS-ARA using GNC
     $\{\hat{\theta}_i\} \leftarrow$ 
        GNCforARA( $\{\tilde{\theta}_{ij}\}, \{\kappa_{ij}\}, \mathcal{E}_{od}, \mathcal{E}_{lc}, c_1, f, \mathbf{A}$ );
    // Convert angle to rotation matrix
     $\{\hat{R}_i\} \leftarrow \text{RecoverR}(\{\hat{\theta}_i\});$ 
    // Solve TLS-TA using GNC
     $\mathcal{I} \leftarrow$ 
        GNCforTA( $\{\hat{R}_i\}, \{\tilde{t}_{ij}\}, \{\tau_{ij}\}, \mathcal{E}_{od}, \mathcal{E}_{lc}, c_2, f, \mathbf{A}$ );
     $\{\tilde{R}_{ij}\} \leftarrow \text{RecoverR}(\{\hat{\theta}_{ij}\});$ 
    // Final estimate
     $(\hat{R}, \hat{t}) \leftarrow$ 
        SE-Sync( $\mathcal{I}, \{(\tilde{R}_{ij}, \tilde{t}_{ij})\}, \{\kappa_{ij}\}, \{\tau_{ij}\}, \mathbf{A}$ );
    return  $\mathcal{I}, (\hat{R}, \hat{t});$ 

```

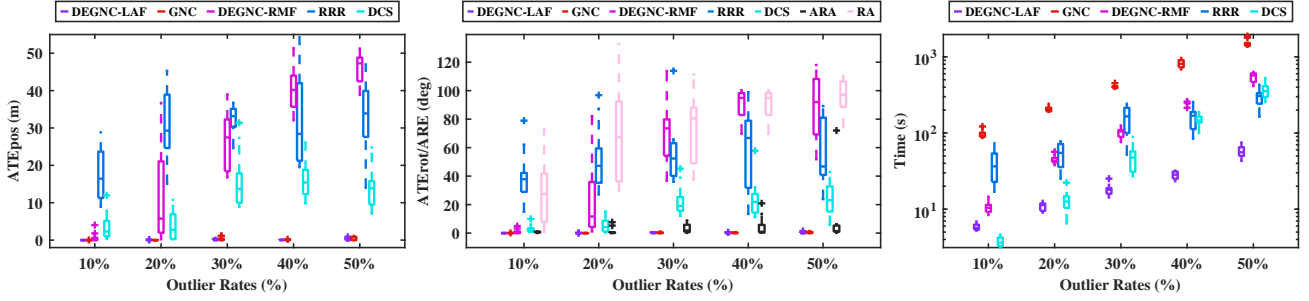


Fig. 1. **city10000** (5000 poses). Average Trajectory Error (ATE), Average Rotation Error (ARE) and the running time of the proposed approach compared to state-of-the-art techniques on the city10000 dataset. Statistics are computed over 10 Monte Carlo runs.

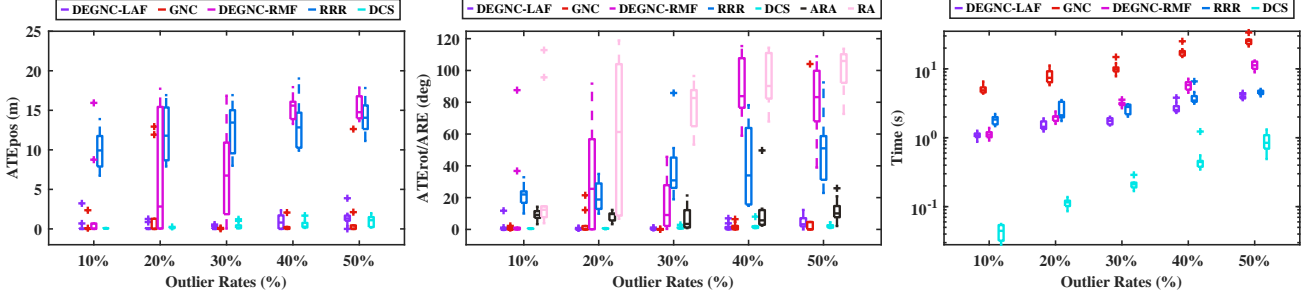


Fig. 2. **intel**. Average Trajectory Error (ATE), Average Rotation Error (ARE) and the running time of the proposed approach compared to state-of-the-art techniques on the intel dataset. Statistics are computed over 10 Monte Carlo runs.

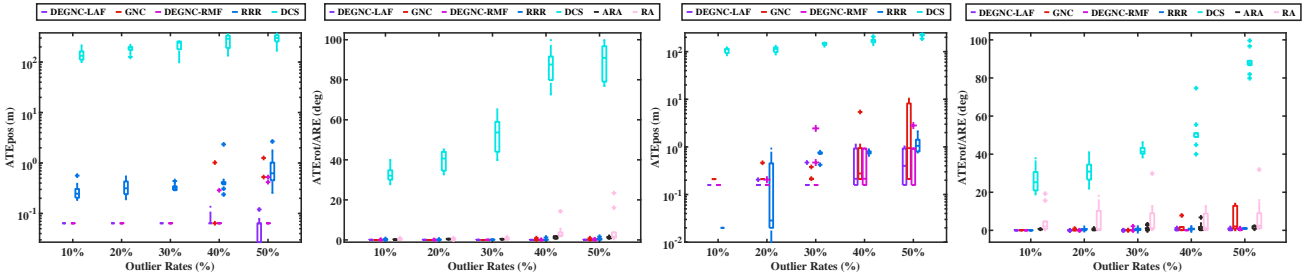


Fig. 3. **kitti.00 and kitti.05**. Average Trajectory Error (ATE) and Average Rotation Error (ARE) of the proposed approach compared to state-of-the-art techniques on the kitti.00 dataset (first to second from left) and the kitti.05 dataset (third to fourth from the left). Statistics are computed over 10 Monte Carlo runs.

TABLE II
INFORMATION OF THE DATASETS TESTED ON

| Dataset | Poses | Loop Closures |
|------------------------|-------|---------------|
| city10000 (5000 poses) | 5000 | 3385 |
| intel | 1728 | 786 |
| kitti.00 | 4541 | 137 |
| kitti.05 | 2761 | 66 |
| manhattan | 3500 | 1953 |

VII. EXPERIMENTS

A. Experimental Setup

We test the performance of DEGNC-LAF on five standard PGO benchmarking datasets: city10000, intel, kitti.00, kitti.05 and manhattan, described in [1]. Some information of these datasets are listed in Table 2. We benchmark our approach against (i) GNC [8], (ii) *DEcoupled GrAduated Non-Convexity with Rotation Matrix Formulation* (DEGNC-BMF), which is the rotation matrix version of DEGNC-LAF (i.e., the first subproblem in the proposed framework is replaced by TLS-ARA with TLS-RA), (iii) *Realizing, Reversing, and Recovering* (RRR) [5] and (iv) *Dynamic Covariance*

Scaling (DCS) [4]. Since GNC takes too much time on the original city10000 dataset, we select only the first 5,000 poses with corresponding measurements of the dataset. However, the datasets we test on contain no outlier initially, so we select random pairs of poses and add a loop closure between each selected pair of poses to simulate outliers.

We performed all experiments in C++ running on a Linux machine with the Intel i7-12700KF (3.60 GHz). We use the latest accelerated version [33] of SE-Sync and SO-Sync (i.e., the rotation averaging version of SE-Sync) to respectively configure GNC and DEGNC-BMF and use 4 threads to drive them, while DEGNC-LAF is implemented with the GTSAM library [34] using only a single thread. The relevant parameters of GNC follow the configuration in [8]. We selected an open source² version of DCS implemented with ceres-solver [17]. We use kernel size $\Phi = 1$ for DCS and 4 threads to drive the ceres-solver, and set the maximum number of iterations to 100, keeping default settings in the source code for all other parameters. We use the RRR algorithm implemented by the authors and set the clustering threshold $\gamma = 10$.

²<https://github.com/gisbi-kim/toy-robust-backend-slam>

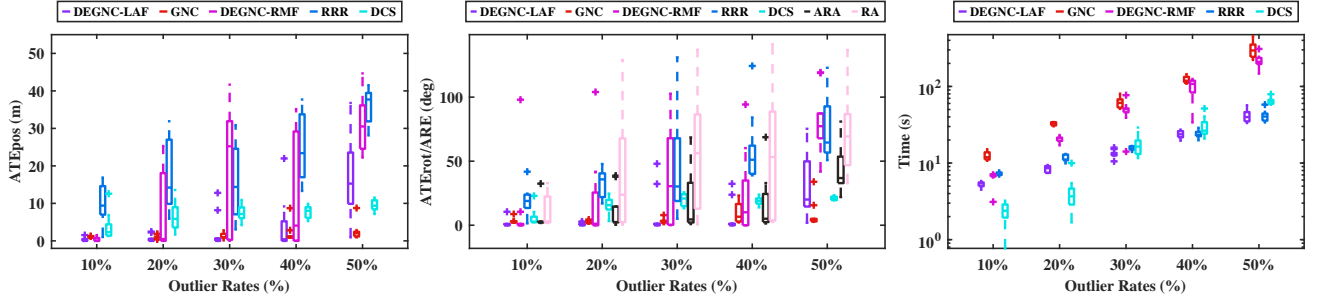


Fig. 4. **manhattan.** Average Trajectory Error (ATE), Average Rotation Error (ARE) and the running time of the proposed approach compared to state-of-the-art techniques on the manhattan dataset. Statistics are computed over 10 Monte Carlo runs.

B. Results

We evaluate the algorithms by Average Trajectory Error (i.e., the ATE_{pos} and ATE_{rot} in [35]) and running time. When evaluating ATE_{rot} we also show Average Rotation Error (ARE) of the solutions to TLS-ARA and TLS-RA with respect to optimal rotation estimates obtained by SO-Sync in the absence of outliers, which are labeled as "ARA" and "RA" respectively in the figures.

city10000. Fig. 1 shows the performance of each algorithm on the city10000 dataset. DEGNC-LAF and GNC dominate other algorithms in terms of accuracy and robustness against outliers. At the same time, DEGNC-LAF is the fastest approach in most cases, except for being slightly slower than DCS at the outlier rate of 10%. Although GNC can achieve similar accuracy to DEGNC-LAF, it is sometimes over 30 times slower than the latter, since it consumes too much time to compute optimality certificates.

intel. Fig. 2 shows the performance of each algorithm on the intel dataset. On this dataset, both DEGNC-LAF and GNC can achieve moderate robustness. Despite this, DEGNC-LAF runs 4-7 times faster than GNC. This dataset allows DCS to maintain more stable performance compared to DEGNC-LAF and GNC and run at a considerable speed. This is probably because the intel dataset provides a good initial guess for DCS so that it does not take a few iterations to reach the global minima.

kitti.00 and kitti.05. These two datasets do not provide initial guesses, so we use the ground-truth as the initial guesses for RRR and DCS. Loop closures in these two datasets are very sparse, so each algorithm can perform good efficiency and thus we do not show the running time in Fig. 3. DEGNC-LAF, GNC and DEGNC-BMF perform good robustness and high accuracy on the kitti.00 dataset. In addition, the solution to TLS-ARA always shows small errors on this dataset. DEGNC-LAF outperforms other algorithms on the kitti.05 dataset, being robust to 50% of outliers, while GNC begins to break at 40% of outliers.

manhattan. manhattan is a particularly challenging dataset for robust planar PGO. The odometry measurements in manhattan have large rotational errors, which causes DEGNC-LAF and DEGNC-BMF to break when solving TLS-ARA and TLS-RA in cases of high outlier rates (e.g., 50%), as shown in Fig. 4. Although GNC shows the best robustness on this dataset, it sometimes falls into local minima and takes hundreds of seconds at high outlier

rates. At outlier rates below 30%, DEGNC-LAF can achieve competitive accuracy with GNC while running 2-4 times faster than the latter and outperforms other algorithms.

C. Discussion

1) *Imperfect accuracy of TLS-ARA:* From the results we can see that the accuracy of solutions to the TLS-ARA problem generally exceeds those of the TLS-RA problem, which can be explained by *Remark 1*. This exhibits the superiority of the angle setting to rotation matrices and ultimately results in better robustness of DEGNC-LAF compared to DEGNC-BMF. Despite the superior accuracy of TLS-ARA, the solutions to TLS-ARA can not always reach perfect accuracy (e.g., as shown in Fig. 2), which explains why we do not directly adopt the solutions to TLS-ARA as the final estimates. Fortunately, the TLS-TA problem is not too sensitive to the rotation accuracy deficiencies caused by TLS-ARA so that it can usually provide a correct set of outliers under mild rotational errors.

2) *Robustness of DEGNC-LAF vs. GNC:* We note that comparing DEGNC-LAF with GNC in terms of robustness presents opposite results on the kitti.05 and manhattan datasets. This can be explained by the fact that the odometry measurements in kitti.05 have low rotational noise but relatively high translational noise, while in manhattan the opposite is true. In scenarios like kitti.05, DEGNC-LAF can obtain a good rotation estimate by solving the first subproblem, allowing the estimation to effectively resist a large number of outliers even with high translational noise, and thus performs better robustness than GNC.

VIII. CONCLUSION

We proposed a specialized framework for global outlier rejection over planar pose graph. Decoupling the TLS-based robust PGO problem and introducing a linear representation for planar rotation are the keys to the proposed framework. This framework requires only linear solvers instead of global nonlinear solvers that require preconditions to reach global optima and are often computationally intensive. We believe the proposed method can be an effective alternative to the standard and general-purpose GNC algorithm for robust planar PGO. This is especially true when the scenario allows for relatively accurate rotation estimation on odometry or when it is necessary to maintain a dense distribution of loop closures.

REFERENCES

- [1] D. M. Rosen, L. Carlone, A. S. Bandeira, and J. J. Leonard, “Se-sync: A certifiably correct algorithm for synchronization over the special euclidean group,” *The International Journal of Robotics Research*, vol. 38, no. 2-3, pp. 95–125, 2019.
- [2] N. Sünderhauf and P. Protzel, “Switchable constraints for robust pose graph slam,” in *2012 IEEE/RSJ International Conference on Intelligent Robots and Systems*. IEEE, 2012, pp. 1879–1884.
- [3] E. Olson and P. Agarwal, “Inference on networks of mixtures for robust robot mapping,” *The International Journal of Robotics Research*, vol. 32, no. 7, pp. 826–840, 2013.
- [4] P. Agarwal, G. D. Tipaldi, L. Spinello, C. Stachniss, and W. Burgard, “Robust map optimization using dynamic covariance scaling,” in *2013 IEEE International Conference on Robotics and Automation*. IEEE, 2013, pp. 62–69.
- [5] Y. Latif, C. Cadena, and J. Neira, “Robust loop closing over time for pose graph slam,” *The International Journal of Robotics Research*, vol. 32, no. 14, pp. 1611–1626, 2013.
- [6] J. G. Mangelson, D. Dominic, R. M. Eustice, and R. Vasudevan, “Pair-wise consistent measurement set maximization for robust multi-robot map merging,” in *2018 IEEE international conference on robotics and automation (ICRA)*. IEEE, 2018, pp. 2916–2923.
- [7] V. Tzoumas, P. Antonante, and L. Carlone, “Outlier-robust spatial perception: Hardness, general-purpose algorithms, and guarantees,” in *2019 IEEE/RSJ International Conference on Intelligent Robots and Systems (IROS)*. IEEE, 2019, pp. 5383–5390.
- [8] H. Yang, P. Antonante, V. Tzoumas, and L. Carlone, “Graduated non-convexity for robust spatial perception: From non-minimal solvers to global outlier rejection,” *IEEE Robotics and Automation Letters*, vol. 5, no. 2, pp. 1127–1134, 2020.
- [9] M. J. Black and A. Rangarajan, “On the unification of line processes, outlier rejection, and robust statistics with applications in early vision,” *International journal of computer vision*, vol. 19, no. 1, pp. 57–91, 1996.
- [10] V. Indelman, E. Nelson, J. Dong, N. Michael, and F. Dellaert, “Incremental distributed inference from arbitrary poses and unknown data association: Using collaborating robots to establish a common reference,” *IEEE Control Systems Magazine*, vol. 36, no. 2, pp. 41–74, 2016.
- [11] A. Karimian, Z. Yang, and R. Tron, “Rotational outlier identification in pose graphs using dual decomposition,” in *European Conference on Computer Vision*. Springer, 2020, pp. 391–407.
- [12] T.-J. Chin and D. Suter, “The maximum consensus problem: recent algorithmic advances,” *Synthesis Lectures on Computer Vision*, vol. 7, no. 2, pp. 1–194, 2017.
- [13] A. Sarlette and R. Sepulchre, “Consensus optimization on manifolds,” *SIAM journal on Control and Optimization*, vol. 48, no. 1, pp. 56–76, 2009.
- [14] P. J. Huber, “Robust statistics,” in *International encyclopedia of statistical science*. Springer, 2011, pp. 1248–1251.
- [15] M. Bosse, G. Agamennoni, I. Gilitschenski, et al., “Robust estimation and applications in robotics,” *Foundations and Trends® in Robotics*, vol. 4, no. 4, pp. 225–269, 2016.
- [16] K. J. Doherty, Z. Lu, K. Singh, and J. J. Leonard, “Discrete-continuous smoothing and mapping,” *arXiv preprint arXiv:2204.11936*, 2022.
- [17] S. Agarwal, K. Mierle, and T. C. S. Team, “Ceres Solver,” 3 2022. [Online]. Available: <https://github.com/ceres-solver/ceres-solver>
- [18] R. Kümmerle, G. Grisetti, H. Strasdat, K. Konolige, and W. Burgard, “g 2 o: A general framework for graph optimization,” in *2011 IEEE International Conference on Robotics and Automation*. IEEE, 2011, pp. 3607–3613.
- [19] R. Hartley and A. Zisserman, *Multiple view geometry in computer vision*. Cambridge university press, 2003.
- [20] P. Antonante, V. Tzoumas, H. Yang, and L. Carlone, “Outlier-robust estimation: Hardness, minimally tuned algorithms, and applications,” *IEEE Transactions on Robotics*, vol. 38, no. 1, pp. 281–301, 2021.
- [21] A. Chatterjee and V. M. Govindu, “Robust relative rotation averaging,” *IEEE transactions on pattern analysis and machine intelligence*, vol. 40, no. 4, pp. 958–972, 2017.
- [22] J. L. Schonberger and J.-M. Frahm, “Structure-from-motion revisited,” in *Proceedings of the IEEE conference on computer vision and pattern recognition*, 2016, pp. 4104–4113.
- [23] J. J. Casafranca, L. M. Paz, and P. Piniés, “A back-end l1 norm based solution for factor graph slam,” in *2013 IEEE/RSJ International Conference on Intelligent Robots and Systems*. IEEE, 2013, pp. 17–23.
- [24] L. Carlone and G. C. Calafiore, “Convex relaxations for pose graph optimization with outliers,” *IEEE Robotics and Automation Letters*, vol. 3, no. 2, pp. 1160–1167, 2018.
- [25] Q.-Y. Zhou, J. Park, and V. Koltun, “Fast global registration,” in *European conference on computer vision*. Springer, 2016, pp. 766–782.
- [26] N. Boumal, A. Singer, P.-A. Absil, and V. D. Blondel, “Cramér–rao bounds for synchronization of rotations,” *Information and Inference: A Journal of the IMA*, vol. 3, no. 1, pp. 1–39, 2014.
- [27] L. Carlone, R. Aragues, J. A. Castellanos, and B. Bona, “A fast and accurate approximation for planar pose graph optimization,” *The International Journal of Robotics Research*, vol. 33, no. 7, pp. 965–987, 2014.
- [28] F. Bai, T. Vidal-Calleja, and G. Grisetti, “Sparse pose graph optimization in cycle space,” *IEEE Transactions on Robotics*, vol. 37, no. 5, pp. 1381–1400, 2021.
- [29] N. Boumal, “An introduction to optimization on smooth manifolds,” *Available online*, May, vol. 3, 2020.
- [30] H. Yang and L. Carlone, “Certifiably optimal outlier-robust geometric perception: Semidefinite relaxations and scalable global optimization,” *IEEE Transactions on Pattern Analysis and Machine Intelligence*, 2022.
- [31] H. Mobahi and J. W. Fisher, “On the link between gaussian homotopy continuation and convex envelopes,” in *International Workshop on Energy Minimization Methods in Computer Vision and Pattern Recognition*. Springer, 2015, pp. 43–56.
- [32] A. Parra, S.-F. Chng, T.-J. Chin, A. Eriksson, and I. Reid, “Rotation coordinate descent for fast globally optimal rotation averaging,” in *Proceedings of the IEEE/CVF Conference on Computer Vision and Pattern Recognition*, 2021, pp. 4298–4307.
- [33] D. M. Rosen, “Accelerating certifiable estimation with preconditioned eigensolvers,” May 2022. [Online]. Available: <https://arxiv.org/abs/2207.05257>
- [34] F. Dellaert, R. Roberts, V. Agrawal, A. Cunningham, C. Beall, D.-N. Ta, F. Jiang, lucacarlone, nikai, J. L. Blanco-Claraco, S. Williams, ydjian, J. Lambert, A. Melim, Z. Lv, A. Krishnan, J. Dong, G. Chen, K. Chande, balderdash devil, DiffDecisionTrees, S. An, mpaluri, E. P. Mendes, M. Bosse, A. Patel, A. Baid, P. Furgale, matthewbroadwaynavenio, and roderick koehle, “borglab/gtsam,” May 2022. [Online]. Available: <https://doi.org/10.5281/zenodo.5794541>
- [35] Z. Zhang and D. Scaramuzza, “A tutorial on quantitative trajectory evaluation for visual(-inertial) odometry,” in *IEEE/RSJ Int. Conf. Intell. Robot. Syst. (IROS)*, 2018.